Sequence-Dependent Nucleosome Structure and Stability Variations Detected by Förster Resonance Energy Transfer†

L. Kelbauskas,‡ N. Chan,‡,§ R. Bash,‡,§,|| J. Yodh,⊥ N. Woodbury,‡,§ and D. Lohr*,§

Biodesign Institute, Department of Chemistry and Biochemistry, and Department of Physics and Astronomy, Arizona State University, Tempe, Arizona 85287, and Division of Basic Sciences, Arizona College of Osteopathic Medicine, Midwestern University, Glendale, Arizona 85308

Received June 27, 2006; Revised Manuscript Received November 8, 2006

ABSTRACT: Nucleosomes, the basic unit of eukaryotic chromosome structure, cover most of the DNA in eukaryotes, including regulatory sequences. Here, a recently developed Förster resonance energy transfer approach is used to compare structure and stability features of sea urchin 5S nucleosomes and nucleosomes reconstituted on two promoter sequences that are nucleosomal in vivo, containing the yeast *GAL10* TATA or the major transcription response elements from the mouse mammary tumor virus promoter. All three sequences form mononucleosomes with similar gel mobilities and similar stabilities at moderate salt concentrations. However, the two promoter nucleosomes differ from 5S nucleosomes in (1) diffusion coefficient values, which suggest differences in nucleosome compaction, (2) intrinsic FRET efficiencies (in solution or in gels), and (3) the response of FRET efficiency to high (≥600 mM) NaCl concentrations, subnanomolar nucleosome concentrations, and elevated temperatures (to 42 °C). These results indicate that nucleosome features can vary depending on the DNA sequence they contain and show that this fluorescence approach is sufficiently sensitive to detect such differences. Sequence-dependent variations in nucleosome structure or stability could facilitate specific nucleosome recognition, working together with other known genomic regulatory mechanisms. The variations in salt-, concentration-, and temperature-dependent responses all occur under conditions that have been shown previously to produce release of H2A−H2B dimers or terminal DNA from nucleosomes and could thus involve differences in those processes, as well as in other features.

The nucleosome is the basic unit of eukaryotic chromosome structure. It is formed by a histone octamer consisting of an H3−H4 tetramer and two H2A−H2B dimers, wrapped by 147 bp of DNA, in slightly fewer than two superturns around the octamer (*1*, *2*). Nucleosomes in vivo can differ in the types of covalent modifications present on the N-terminal histone tails (*3*−*5*) and in the presence of histone variants (*3*, *6*). The presence of variant histones is able to create structural differences in nucleosomes. For example, H2A variant H2A.Z, which is enriched in heterochromatin, makes nucleosomes more salt stable (*7*), and variant H2A.Bbd, which is proposed to be associated with transcriptionally active chromatin, causes less than the canonical length of DNA to be wrapped around an octamer containing it (*8*). The ability of specific histone variants to alter nucleosome properties could help make specific nucleosomes or nucleosomal regions distinctive and thus identifiable within the genomic population.

DNA sequence-dependent variations are another obvious potential source of nucleosome differences. Eukaryotic DNA is thought to be extensively covered by nucleosomes in vivo (*9*), including regulatory elements like gene promoters (*10*−*14*) and replication origins (*15*−*17*). Sequence-dependent variations in nucleosome structure could endow nucleosomes at specific DNA sites with unique properties that aid in their recognition or alteration by established regulatory mechanisms (*3*, *4*, *18*).

Indeed, there are known DNA sequence-associated variations in some nucleosome features, such as reconstitution efficiencies (*19*−*22*), nucleosome occupancy of promoter DNA in vivo and in vitro (reviewed in ref *23*), nucleosome repositioning and Swi-Snf remodeling (*20*, *24*, *25*), the contributions of histone tails to nucleosome stability (*26*), torsional and dynamic properties of nucleosomal DNA (*20*, *27*, *28*), and the forces required to unravel nucleosomes (*29*). Obviously, it would be of great interest to develop a system that can sensitively explore sequence-associated variations for a wide range of intrinsic nucleosome features.

We have recently developed a FRET[1]-based approach that can monitor nucleosome conformational features (*30*). FRET is a powerful approach for the study of conformational

† This work was supported by National Institutes of Health Grant CA85990 (D.L.) and National Science Foundation Grant PHY-0239986 (to N.W. and D.L.).

* To whom correspondence should be addressed. E-mail: DLohr@asu.edu.

‡ Biodesign Institute, Arizona State University.

§ Department of Chemistry and Biochemistry, Arizona State University.

|| Department of Physics and Astronomy, Arizona State University.

⊥ Midwestern University.

[1] Abbreviations: FRET, Förster resonance energy transfer; FCS, fluorescence correlation spectroscopy; MMTV, mouse mammary tumor virus; PCR, polymerase chain reaction; GR, glucocorticoid receptor; CCD, coupled charge device.

10.1021/bi061289l CCC: $37.00 © 2007 American Chemical Society
Published on Web 02/01/2007

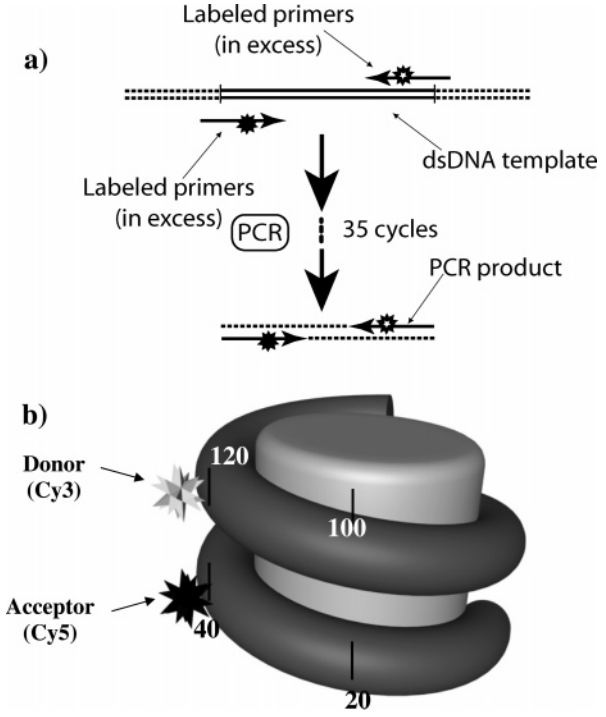

FIGURE 1: FRET-labeled nucleosomes. Panel a shows how the DNA fragments used in this study (5S, MMTV, and *GAL10*) were labeled with Cy3 and Cy5 fluorophores at sites 80 bp apart. PCR was performed with DNA template fragments and appropriate sequence primers with Cy3 or Cy5 at sites ~40 bp from each end. After ~35 cycles, the product is mainly full-length (~160 bp) doubly labeled dsDNA, which is then gel purified. Panel b illustrates how the wrapping of DNA in a canonical nucleosome will place FRET donor and acceptor sites that lie 80 bp apart on a DNA fragment close enough to permit high-efficiency energy transfer when the DNA is reconstituted into a nucleosome. Conformational changes that significantly alter the donor−acceptor distance will result in changes in energy transfer efficiency. The stars represent fluorophores Cy3 and Cy5.

changes in biological macromolecules, and it can be used in various ways (*31*−*43*). Energy transfer (FRET) occurs when an excited donor fluorophore is in the proximity (~1−5 nm) of an appropriate acceptor fluorophore. Because the efficiency of energy transfer depends on the sixth power of the donor−acceptor distance, FRET is very sensitive to distance changes between the donor and acceptor, for example, the types of changes occurring during conformational transitions in biomolecules. FRET approaches can be used in combination with fluorescence correlation spectroscopy (FCS) techniques to determine diffusion coefficients, which provide insights into the shape properties of complex biomolecules.

Our approach involves labeling a DNA fragment with the donor fluorophore, Cy3, and an acceptor fluorophore, Cy5, at sites 80 bp apart on the DNA sequence ("PCR product", Figure 1a). When this labeled DNA is reconstituted into nucleosomes, the donor and acceptor are brought close enough, by the nucleosomal wrap (Figure 1b), to produce efficient energy transfer and a strong FRET signal when the donor is excited (*30*). This system is a sensitive monitor of nucleosome conformational changes, such as those induced by salt (*30*) or by the action of ATP-dependent nucleosome remodeling complexes (L. Kelbauskas et al., unpublished observations). These labeled nucleosomes are also appropriate for single-molecule studies (*30*, *44*).

Here we use this approach to study the intrinsic properties of nucleosomes reconstituted on three natural DNA sequences, a TATA-containing sequence from the yeast *GAL10* promoter (*45*), a crucial regulatory sequence (MMTV-B) from the MMTV promoter (*46*), and a fragment from the sea urchin 5S rDNA gene (*47*). The *GAL10* and MMTV-B fragments were chosen because they are examples of in vivo sequences that reside in nucleosomes in the inactive transcriptional state but undergo significant structural changes in association with gene activation. For example, MMTV nucleosome B, which contains four of the six glucocorticoid receptor (GR) binding sites on this promoter, undergoes a structural transition that is crucial to the GR-induced gene activation process (*46*). The 5S rDNA sequence is probably the most widely used model for both mononucleosome and nucleosomal array studies (*48*) and provides a standard of comparison for the other two sequences. All three sequences exhibit at least some ability to position nucleosomes (*12*, *20*, *45*, *49*−*52*).

In the work described below, we analyze several basic features of mononucleosomes reconstituted on the three sequences mentioned above. The goal is to use the power and sensitivity of FRET approaches to test the hypothesis that DNA sequence-associated effects can cause clear and detectable variations in nucleosome structure and stability. This will involve comparing nucleosomes made with these three DNA sequences but fluorescently labeled in the same way, reconstituted with the same histones, and analyzed in exactly the same way. The features that were analyzed include diffusion coefficients (by FCS) and intrinsic FRET efficiencies, both of which should monitor structural features, and variations of FRET efficiency as a function of NaCl concentration, nucleosome concentration, and temperature (up to 42 °C), which should monitor various facets of nucleosome stability. All three sequences form nucleosomes that are similar in some ways (gel mobilities and stabilities to moderate NaCl concentrations) but clearly different in others [diffusion coefficients, intrinsic FRET efficiencies, and FRET efficiency variations in response to nucleosome dilution, temperature increase (42 °C), and high (≥600 mM) NaCl concentrations]. These results show that nucleosome structure and stability features can vary with DNA sequence and that these FRET approaches are sufficiently sensitive to permit detection of such variations.

MATERIALS AND METHODS

DNA and Nucleosome Preparation. The fluorescently labeled dsDNA fragments were made by PCR, using two labeled primers and the appropriate template DNA as illustrated in Figure 1a (see also ref *30*). The template for preparing the 160 bp *GAL10* fragment was a 907 bp *GAL 1*−*10* promoter fragment (*53*), and the two primers that were used were biotin-5′-ttctaatccgtacttcaatatagcaatgagcagttaagcgtatXactgaaagttccaaag-3′ and 5′-attacatggcattaccaccatatacatatccatatcXaatcttacttatatgttgtggaa-3′. The template for preparing the 160 bp MMTV B fragment was the 6115 bp pGEM3ZFM-LTRCAT fragment that contains an MMTV promoter fragment (*54*); the two primers were biotin-5′-ttggcccaaccttgcggttcccaaggcttaagtaagttttt-ggtXacaaactgttcttaa-3′ and 5′-ataaattccaaaagaacataggaaaatag-aacacXcagagctcagatcagaacctttgat-3′. The template for making the 154 bp sea urchin 5S rDNA fragment [which corresponds

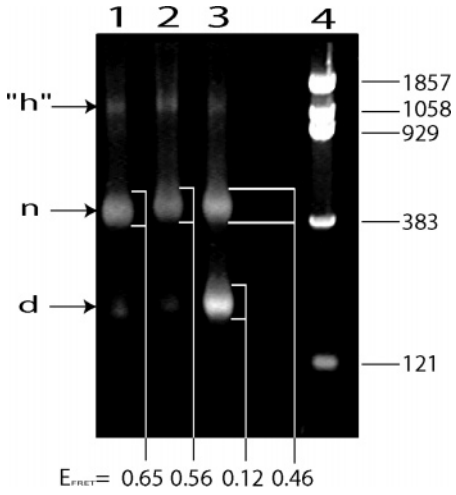

FIGURE 2: Gel analyses of reconstituted nucleosome samples. Reconstituted 5S (track 1), MMTV-B (track 2), and *GAL10* (track 3) nucleosome samples were run on a polyacrylamide gel, with pBR-BstN1 DNA markers (track 4 with band sizes given at the right). The labels d, n, and h identify free DNA, the mononucleosome band, and higher-molecular weight components (see the text), respectively. The fractional numbers below the gel are the FRET efficiencies for the specific mononucleosome bands and one free DNA band measured directly in the gel (see the text). The samples for in-gel analysis were the same ones whose ethidium bromide profiles are shown here, run on the same type of gel but not stained with ethidium bromide.

to the region between the 5′ *Eco*RI restriction site and the *Ban*II restriction site (*51*)] was a 195 bp *Eco*RI−*Eco*RI fragment; the two primers were biotin-5′-ccaacgaataacttc-cagggatttataagccgaXgacgtcataacctccctgacccttta-3′ and 5′-agc-cctatgctgcttgacttcggtgatcggacgagaaccggtataXtcagcatggtatgg-3′ [note that for historical reasons in the lab, a slightly altered (1 bp difference) 5S rDNA sequence was used in these studies, compared to the original reference]. In all the primers that were used, X represents a thymine-labeled base with either Cy3 (first primer) or Cy5 (second primer). Primers were obtained from IBA GmbH (Göttingen, Germany).

After labeling had been carried out, the DNA was gel-purified and reconstituted into nucleosomes with purified HeLa octamer histones or recombinant *Xenopus laevis* octamer histones using salt-step dialysis, as described previously (*55*), with the exception that the final buffer for dialysis was 10 mM HEPES (pH 7.8) instead of 1 mM EDTA (pH 8.0). The preparation of HeLa histones has been previously described (*56*); *Xenopus* histones were obtained from Upstate (Charlotesville, VA) and renatured as described in ref *57*. The histone:DNA ratios that gave mostly mononucleosomes, with little free DNA or higher bands on polyacrylamide gels, were empirically determined.

The primers were chosen so that the fluorophores would be located roughly 30 bp from each terminus in the reconstituted nucleosome, based on in vitro nucleosome positioning data for the 5S sequence (*51*, *52*), in vivo and in vitro nucleosome positioning data for the MMTV-B sequence (*12*, *54*, *58*), and in vivo nucleosome positioning data for the *GAL10* sequence (cf. ref *45*). For each of these sequences, one major nucleosome position was observed (Figure 2), despite previous reports of positioning heterogeneity [5S (*51*) or MMTV (*12*, *58*)].

Bulk FRET Measurements and Salt Titrations. Bulk solution fluorescence emission spectra were recorded on a home-built fluorimeter consisting of a xenon lamp as the excitation source, excitation and emission monochromators (SpectraPro-150, Acton Research, Dayton, OH), a sample holder, and a CCD array detector (NTE/CCD-1340/100-EMB..FG, Princeton Instruments, Monmouth Junction, NJ). Quartz microcuvettes with covers (16.40F-Q-10/Z15, Starna Cells, Inc., Atascadero, CA) were used to measure the fluorescence intensity of 100 μL samples excited at 515 nm.

For the salt titrations, emission spectra were recorded for both the sample and a control with reference naked DNA (the same 5S rDNA was used throughout), and then an appropriate volume of 5 M NaCl was added to the nucleosome sample and the sample allowed to equilibrate for 30 min [the time required to allow equilibrium, i.e., steady level of FRET, to be achieved (*30*)]. Then the emission spectra of the nucleosome sample and the DNA reference were measured again. Addition of salt (to the nucleosome sample) was continued until there was no longer a detectable Cy5 peak in the emission spectrum. Cy5:Cy3 ratios for the nucleosome sample were corrected for lamp intensity fluctuations (determined from the reference DNA emission values) and for volume changes due to salt addition.

Measuring Concentration and Temperature Dependence of FRET and FRET Efficiency of Gel Bands. FRET measurements as a function of concentration or temperature were conducted using a microscope (ECLIPSE TE2000-U, Nikon, Melville, NY) operated in a confocal configuration. An intracavity frequency-doubled CW Nd:YVO_4 laser (Millenia Xs, Coherent, Santa Clara, CA) operating at 532 nm was used as the excitation source. The excitation beam was focused, and the fluorescence was collected using a 100× oil-immersion objective lens with a numerical aperture of 1.4 (Plan Apo 100×/1.40 Oil, Nikon, Melville, NY). The emission photons were separated into the donor and acceptor channel by a dichroic mirror (Chroma Technology Corp., Rockingham, VT). The photons in each channel were detected with silicon avalanche photodiodes (SPCM-AQR-12, Perkin-Elmer, Fremont, CA) using emission filter sets designed for Cy3 or Cy5 emission placed in front of each detector. The signals were recorded using a data acquisition card (DAQ-6017, National Instruments, Austin, TX), and the data analysis was performed using home-written software based on LabView (version 7.1, National Instruments). The concentration and temperature dependence measurements were carried out in 10 mM Tris and 1 mM EDTA buffer with the pH adjusted to 8. The temperature was adjusted using an objective heater (Bioptech, Butler, PA). For fluorescence measurements of bands in polyacrylamide gels, the same experimental arrangement equipped with a 20×, NA = 0.5 objective lens (Plan Fluor 20×/0.50, Nikon) was used. For all experiments, the FRET efficiency was calculated using the standard equation

$$E_{\mathrm{FRET}} = \frac{I_{\mathrm{A}}}{I_{\mathrm{A}} + \gamma I_{\mathrm{D}}} \qquad (1)$$

where I_{A} and I_{D} are the fluorescence intensities measured in the acceptor and donor channel, respectively, and γ is a factor correcting for the cross talk between the detection channels and direct acceptor excitation contributions.

Controls. It is possible that increases in temperature or salt concentration may affect the basic emission properties

of fluorophores like Cy3 and Cy5. Such effects could produce changes in the FRET signal that could be misinterpreted as a conformational change reflecting alterations in the donor−acceptor distance on the nucleosome. To account for possible temperature and salt effects on the dyes, control measurements were conducted under the same experimental conditions using nucleosomes singly labeled either with Cy3 or Cy5 at the same DNA positions as on the doubly labeled nucleosomes. We measured the emission intensity dependence on temperature (20−42 °C) and NaCl concentration (0−1.6 M) of Cy3-only and Cy5-only labeled nucleosomes. The results showed that the emission intensity of both dyes, Cy3 and Cy5, decreases at nearly equal rates with a temperature increase. This is what one would expect; Cy3 and Cy5 dyes have similar molecular structure, and it is reasonable that temperature and salt should have similar effects on the emission properties of both dyes. Because of this, the emission intensity changes due to temperature or salt should cancel each other when FRET efficiency is calculated (see eq 1). The calculated relative change in FRET efficiency resulting from the temperature effect on the dyes is <2% at 40 °C and <1% at 30 °C. The emission intensity dependence on NaCl concentration also revealed a nearly identical behavior of Cy3- and Cy5-only labeled nucleosomes. The resulting relative change in the FRET signal due to NaCl concentration was calculated to be <2% in the concentration range between 600 and 1600 mM and <0.5% in the range of 0−400 mM. The results show that both temperature and NaCl effects on Cy3 and Cy5 dyes can be neglected when the relative quantity, FRET efficiency, is calculated.

Fluorescence Correlation Spectroscopy (FCS) Measurements. FCS measurements were carried out using the same experimental setup as described above. Correlation curves were measured using a hardware dual-channel digital correlator with a sample time of 12.5 ns (Flex2k-12x2, Correlator, Bridgewater, NJ) and the vendor's software. The analysis was performed using home-written software based on LabView (version 7.1, National Instruments). For all measurements, the nucleosome and free DNA concentrations were in the subnanomolar range. The cross correlation results were generated through simultaneous analysis of the donor (Cy3) and acceptor (Cy5) channels. In this way, detector afterpulsing effects that often occur in uncorrected autocorrelation traces were avoided. Performing cross correlation also ignores any contributions from free (non-nucleosomal) DNA. The data were fit to a single-component free three-dimensional diffusion model using the equation (*59*)

$$G(\tau) = \frac{1}{N}\frac{1}{1+\frac{4D\tau}{r_0^2}}\frac{1}{\left(1+\frac{4D\tau}{z_0^2}\right)^{1/2}} \qquad (2)$$

where N is the average number of molecules in the detection volume, D is the diffusion constant, and r_0 and z_0 are the radial and axial radii of the detection volumes, respectively. During the fit, N and D were varied freely, whereas r_0 and z_0 were kept fixed. The radial and axial radii were determined from an independent measurement using fluorescent beads of a known size as a reference.

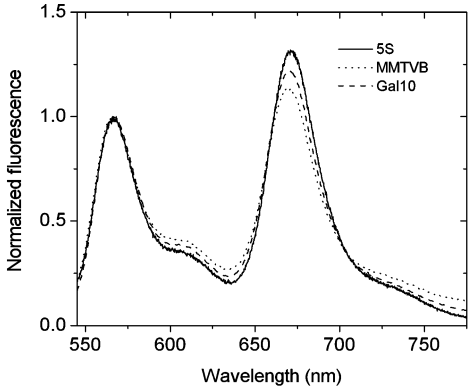

FIGURE 3: Bulk fluorescence. The bulk solution fluorescence emission spectra for 5S, MMTV-B, and *GAL10* nucleosome samples are shown. Excitation was carried out at 515 nm. The peak at ~570 nm corresponds to the Cy3 (donor) emission maximum, and the peak at ~670 nm is the Cy5 (acceptor) emission maximum. Spectra were normalized to one another at the Cy3 emission maximum value. The 5S and MMTV-B samples are the same ones shown in Figure 2. The *GAL10* sample is shown in the inset of Figure 4a.

RESULTS

Gel Characterization. Figure 2 shows polyacrylamide gel profiles of the three types of reconstituted samples, 5S (track 1), MMTV-B (track 2), and *GAL10* (track 3). The mobilities of the three mononucleosome bands ("n") relative to DNA markers (track 4) or to the naked DNA fragments used in the reconstitution ("d") are typical for mononucleosomes on these types of gels, indicating that all three form typical nucleosomes. The mobilities of the three are also similar. On these types of gels, reconstituted samples can exhibit multiple bands in the mononucleosome region, reflecting heterogeneity in nucleosome positioning on the DNA, and small amounts of intensity at higher positions, which is thought to reflect two nucleosomes on a single DNA fragment (*60*, *61*). Other, minor bands in the mononucleosome region are occasionally observed in our samples, but this is not common. Minor amounts of higher-molecular weight material are usually present to a similar extent in all three types of samples ("h", Figure 2). The significant amount of free DNA in the *GAL10* sample shown in Figure 2 was useful for an analysis carried out on these samples (see below) but is not characteristic of the *GAL10* samples used in this work (for example, see the inset of Figure 4a).

Bulk FRET Measurements. Figure 3 shows bulk solution emission spectra for the three types of labeled nucleosomes. The donor (Cy3) emission maximum is at 570 nm, and the acceptor (Cy5) emission maximum is at 670 nm. The peak positions and general shape of the spectra are similar, indicating that in all three nucleosomes, the two fluorophores have similar photophysical properties. Excitation is at 515 nm, a wavelength at which Cy5 emission due to direct excitation is negligible. Thus, the ratios of Cy5:Cy3 peak intensities in these spectra reflect the efficiency of energy transfer; the higher the ratio, the more efficient the transfer.

The Cy5:Cy3 ratio is highest for the 5S sample and lower for MMTV-B and *GAL10*. The same trend is seen in the composite data set, i.e., the entire set of reconstituted nucleosome samples of each type analyzed in this work (Table 1). Differences in the efficiency of DNA labeling do not explain these results; 5S DNA is typically a bit less

Table 1: Composite FRET and FCS Values[a]

nucleosome type	bulk solution Cy5:Cy3 ratio[b]	FRET efficiency in solution[d]	FRET efficiency in gel[e]	diffusion coefficient ($\mu m^2/s$)[f]
5S	1.5 ± 0.2	0.52 ± 0.03	0.66 ± 0.01	21 ± 1
MMTV	1.1 ± 0.1	0.38 ± 0.04	0.57 ± 0.04	15 ± 1
GAL10	1.0 ± 0.1 (1.1 ± 0.1)[c]	0.37 ± 0.03	0.49 ± 0.03	15 ± 1

[a] All error values were calculated as the standard error of the mean. [b] Value of the Cy5:Cy3 emission ratio in bulk measurements in the fluorimeter (cf. Figure 3). [c] Average value at 200 mM NaCl. [d] Energy transfer efficiency measured at initial concentrations (cf. Figure 4) or 25 °C (cf. Figure 5) in the concentration and temperature experiments. [e] Energy transfer efficiency measured directly on bands in gels (cf. Figure 2). [f] Average values of diffusion coefficients from FCS measurements (cf. Figure 6).

efficiently labeled than the other two DNAs (based on analysis of the absorbance spectrum of the gel-purified PCR products). The 5S and MMTV-B spectra in Figure 3 are from the samples shown in Figure 2, and the *GAL10* spectrum is from the sample whose gel profile is shown in the inset of Figure 4a. The large amounts of free DNA, which have Cy3 emission but no possibility for energy transfer (*30*), would skew the Cy5:Cy3 ratio (underestimating the FRET efficiency) if the *GAL10* sample in Figure 2 were used.

We also measured FRET efficiencies for the mononucleosome and free DNA bands directly in gels, using a scanning microscope; these are the numbers shown below the gel in Figure 2. FRET efficiency is highest for the 5S mononucleosome (0.65) and lowest for the *GAL10* mononucleosome (0.46). Efficiency for the MMTV-B mononucleosome falls between the other two values (0.56). The FRET efficiency in the free DNA band is ~0.12. Again, composite values show the same trend: 5S > MMTV > *GAL10* (Table 1). Thus, in-gel analyses, which specifically analyze the mononucleosome band, also detect energy transfer efficiency differences for the three types of nucleosomes, as suggested by bulk solution results. FRET efficiency differences reflect variations in the average distance between the two fluorophores in the nucleosome structure. Thus, there are structural variations among the three types of nucleosomes even though their gel mobilities, and thus their gross structures, are similar.

Salt Stability. The salt stability for these three types of nucleosomes was characterized by monitoring the Cy5:Cy3 ratio as the salt concentration was increased from initial low values (~1 mM). Figure 4a shows an example of such a response ("titration") for the *GAL10* sample shown in the inset. The Cy5:Cy3 ratio increases slightly as the NaCl concentration is increased from 1 to 200 mM and then progressively decreases as the concentration is increased above 200 mM. By 1000 mM NaCl, the Cy5:Cy3 ratio, and thus energy transfer, is <10% of the low-salt values.

To facilitate comparisons among the three types of samples, composite titration curves were generated (Figure 4b). By averaging over all the determinations for a given type of nucleosome sample, this approach can take into account experiment-to-experiment and sample-to-sample variations. To make such a curve, the Cy5:Cy3 ratio was set to 1.0 at the lowest NaCl concentration, and the Cy5:Cy3 ratios at higher NaCl concentrations were normalized against this value to generate a normalized titration curve

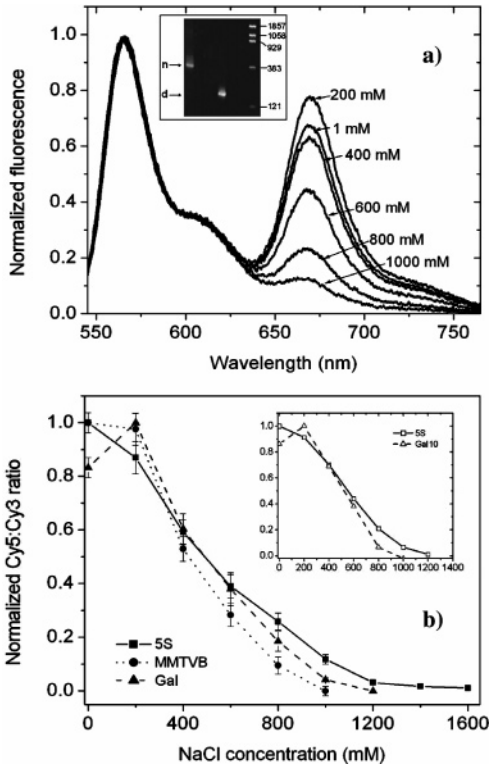

FIGURE 4: Salt titrations. In panel a, an example of a salt titration, i.e., the change in emission spectra with an increase in NaCl concentration, is presented for a *GAL10* nucleosome sample. The various salt concentrations at which spectra were recorded are identified. All were normalized to the Cy3 peak emission. The sample is shown in the leftmost track of the inset gel. The other tracks in that gel contain, from left to right, a *GAL10* free DNA sample, d, and DNA markers (numbers denote size in base pairs). Panel b shows plots of the normalized Cy5:Cy3 ratio, obtained from individual salt titrations such as the one in panel a, for 5S (■), MMTV-B (●), and *GAL10* (▲) samples. Each curve shown is a composite, the average of all the individual titrations done for that type of sample, i.e., various reconstitutes and various trials for each reconstitute (see the text). The inset shows composite titration curves of 5S and *GAL10* nucleosomes reconstituted with recombinant *Xenopus* histones [5S (□) and *GAL10* (△)].

for an individual sample. Then these individual normalized curves were averaged together to generate the composite curve for that type of nucleosome. Note that this approach largely removes the influence of free DNA present in the sample. These titrations have been carried out carefully, with internal controls (see Materials and Methods), and multiple samples were analyzed in multiple trials, for each type of sample. Thus, the differences described below are statistically significant (Figure 4b).

The three composite salt titration curves are roughly similar, indicating that the salt stabilities of the three types of nucleosomes are similar. However, there are some differences. In the range from 600 to 1000 mM, 5S nucleosome samples retain higher energy transfer (Cy5:Cy3) levels and are therefore somewhat less sensitive to salt disruption than *GAL10* or MMTV nucleosome samples. For example, 5S Cy5:Cy3 ratios fall below 10% of their initial value at NaCl concentrations of >1000 mM, whereas *GAL10* ratios do so by ~900 mM and MMTV ratios by 800 mM. Thus, MMTV and *GAL10* nucleosomes more easily undergo a change that results in FRET decreases, i.e., at lower NaCl concentrations, than 5S nucleosomes. These ratio decreases at high salt concentrations must reflect changes in nucleo-

some conformation because formaldehyde or glutaraldehyde-cross-linked *GAL10*, MMTV, or 5S nucleosomes maintain high energy transfer levels (Cy5:Cy3 ratios) even at 1 M NaCl (data not shown). Thus, the differing responses of these three types of nucleosomes suggest stability differences above 600 mM NaCl.

There are also variations in the FRET response between 1 and 200 mM (Figure 4b). Most noticeably, the FRET level actually increases between 1 and 200 mM NaCl for the *GAL10* nucleosome sample, whereas the FRET level is constant for MMTV and decreases for 5S in this salt range. Most of the *GAL10* increase has occurred by 50 mM NaCl (L. Kelbauskas et al. unpublished observations). These variations may reflect differential tendencies to undergo the types of nucleosome conformational changes detected previously in these low salt ranges using other approaches and mixed sequence nucleosomes purified from cells (*62*, *63*). Note that the maximum Cy5:Cy3 ratio for *GAL10* nucleosomes, i.e., at 200 mM NaCl, is still significantly lower than the maximum Cy5:Cy3 ratio for 5S nucleosomes (Table 1). In sum, these salt titration results indicate that all three types of nucleosomes have roughly similar salt stabilities and thus must form roughly similar nucleosomes, consistent with the gel mobility results, but there are some salt-dependent stability variations among the three.

We tested the histone dependence of the salt stability differences by reconstituting 5S and *GAL10* nucleosomes with *Xenopus* (recombinant) histones instead of human histones. The inset of Figure 4b shows that the same differences are observed, a FRET increase between 1 and 200 mM NaCl in *GAL10* but not 5S nucleosomes and a decreased FRET level (decreased stability) above 600 mM in *GAL10* relative to 5S. Thus, these salt stability differences are independent of histone type. Since recombinant histones lack histone tail modifications, this result also excludes any contribution of such modifications to the observed differences.

Temperature Dependence of FRET. As nucleosomes are heated to 40−45 °C, the ∼20 bp of DNA near each terminus is released from the nucleosome (*64*). These terminal regions have relatively fewer DNA−histone contacts, and the DNA would be expected to be preferentially released from these regions (*65*). Thus, we have monitored the temperature dependence of the FRET signal in this temperature range for the three types of nucleosomes.

Figure 5 shows temperature profiles of the energy transfer efficiencies up to 42 °C, the upper temperature limit for our experimental setup. As the temperature is increased to 42 °C, the FRET efficiency values for the MMTV and *GAL10* nucleosome samples fall by 20−30% whereas the 5S values remain high. Thus, on the basis of these FRET efficiency changes, 5S nucleosomes respond differently than MMTV and *GAL10* nucleosomes to this temperature increase. The FRET level decrease in MMTV and *GAL10* nucleosomes is only partial, falling to at most 70% of the value at 25 °C (for *GAL10*), showing that the *GAL10* and MMTV-B nucleosomes are still sufficiently intact to produce strong energy transfer at 42 °C. A partial FRET change is consistent with a partial change in nucleosome structure, such as release of terminal DNA. Decreases of 20−30% in FRET efficiency (MMTV-B and *GAL10*) correspond to relatively small average increases in interprobe separation (see Discussion).

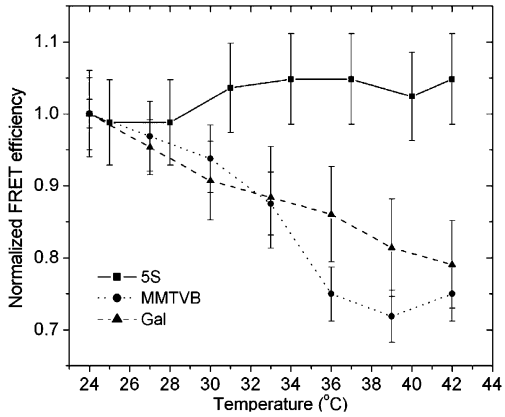

FIGURE 5: FRET efficiency as a function of temperature. 5S (■), MMTV-B (●), and *GAL10* (▲) nucleosome samples were diluted to similar subnanomolar concentrations in 10 mM Tris with 1 mM EDTA buffer at pH 8.0, and the temperature of the solution increased progressively. FRET efficiency was determined from the fluorescence intensities in the Cy3 and Cy5 detection channels (see Materials and Methods) at each temperature that is shown.

Control measurements of singly labeled nucleosomes have shown that any temperature-dependent effects on the properties of the dyes themselves do not affect the FRET signal significantly (see Materials and Methods).

The slight increase in FRET efficiency with temperature for 5S nucleosomes is consistently observed. We have found that at temperatures around 40 °C, 5S nucleosomes are in a state that produces a higher level of FRET but is less salt-stable (L. Kelbauskas et al., manuscript in preparation). Thus, instead of undergoing the types of changes that reduce the FRET efficiencies of MMTV and *GAL10* nucleosomes at ∼40 °C, 5S nucleosomes go into a state with slightly enhanced FRET (compared to ambient conditions). This is another behavioral difference. The 5S and MMTV samples are those shown in Figure 2; the *GAL10* sample shown is similar (gel profile etc) to those.

Concentration-Dependent Stability. An important consideration for single-molecule studies is the stability of the nucleosome to dissociation. Both histone−histone [H3−H4 tetramers from H2A−H2B dimers (*2*)] and DNA−histone dissociation (partial or complete) can take place in nucleosomes. To monitor this aspect of stability, we measured the FRET efficiency for these three nucleosome samples as a function of concentration, by serial dilution studies (Figure 6).

FRET efficiencies for 5S nucleosome samples remain high down to 100 pM levels, whereas MMTV and *GAL10* nucleosomes show a decrease in FRET efficiency with dilution. The *GAL10* decrease is consistently greater than the MMTV decrease, but even it is only partial, falling at most to ∼65% of the initial values. Thus, as for the temperature changes, these concentration-dependent changes must reflect only a partial change in the nucleosome, not its complete disruption. The 5S and MMTV samples are the same ones shown in Figure 2; the *GAL10* sample is similar (gel profile) to those samples. The slight increase in FRET efficiency with dilution for the 5S sample is a consistent observation. It may reflect a transition to a structure with a slightly higher FRET efficiency, as for the temperature response (above).

FCS Studies. FCS measurements were carried out to determine diffusion properties for the three types of nucleo-

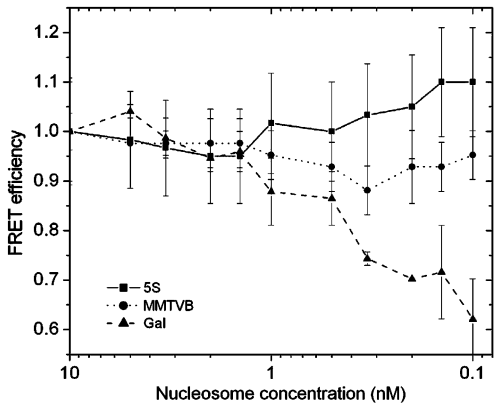

FIGURE 6: FRET efficiency as a function of nucleosome concentration. 5S (■), MMTV-B (●), and *GAL10* (▲) nucleosome samples were suspended in 10 mM Tris with 1 mM EDTA buffer at pH 8.0 at the same initial nucleosome concentrations of 10 nM, as determined from absorbance measurements. Then they were successively diluted in the same buffer, and the FRET efficiency was determined from the fluorescence intensities in the Cy3 and Cy5 detection channels (see Materials and Methods).

somes in solution, to gain insight into this aspect of nucleosome conformation. An example of raw cross correlation data and a theoretical fit to the data (see Materials and Methods) are shown in Figure 7a, and curves showing examples of data fits for all three types of nucleosomes as well as naked DNA (donor channel autocorrelation) are shown in Figure 7b. Both the specific results presented in Figure 7b and composite results (Table 1) show that 5S nucleosomes have a higher diffusion coefficient than MMTV and *GAL10* nucleosomes, which both have similar values. The data presented in Figure 7b are from the same three samples shown in Figure 2 (the presence of free DNA has no effect on FCS cross correlation values; see Materials and Methods). Diffusion coefficients for 5S nucleosomes average $21 \pm 1\ \mu m^2/s$, versus $15 \pm 1\ \mu m^2/s$ for *GAL10* and MMTV nucleosomes. Since the lengths of DNA used to reconstitute these nucleosomes are similar and the same histones were used in the reconstitution, this result indicates that the 5S nucleosomes are somewhat more compact than MMTV and *GAL10* nucleosomes. The diffusion coefficients for naked DNA are typically smaller (cf. Figure 7b). Note that for these studies, the important data are the relative diffusion coefficient values, not the absolute values.

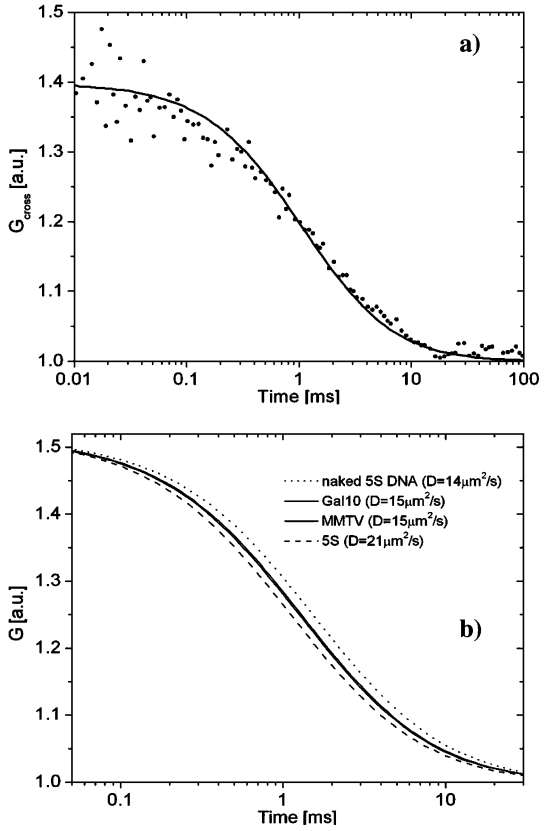

FIGURE 7: FCS studies. Panel a shows an example of a cross correlation experiment between the Cy3 and Cy5 detection channels, with data shown in dots and a theoretical fit to the data (single-component three-dimensional free diffusion model; see Materials and Methods) shown as a solid line, for a 5S nucleosome sample. In panel b, fits to fluorescence autocorrelation data for free 5S DNA (···) and Cy3−Cy5 cross correlation data for 5S (- - -), *GAL10*, and MMTVB (—) nucleosome samples are shown. The nucleosome and free DNA concentrations were ∼0.1 nM. The diffusion coefficients for the nucleosomes are determined from the fit (see Materials and Methods).

DISCUSSION

Mononucleosomes were reconstituted on three physiologically relevant DNA sequences, *GAL10*, MMTV-B, and 5S. In each case, an ∼160 bp DNA fragment was labeled with donor (Cy3) and acceptor fluorophores (Cy5) at sites 80 bp apart, bracketing the center of the fragment (Figure 1a). Reconstitution of nucleosomes with such labeled DNA brings the donor and acceptor into spatial proximity (Figure 1b), producing strong energy transfer when the donor is excited. This probe system is a sensitive reporter of nucleosome conformation (*30*).

The *GAL10* and MMTV-B sequences contain the TATA motif (*GAL10*) and four of the six elements that mediate hormone induction of MMTV gene expression (MMTV-B) from their respective pol II promoters. They were chosen because the nucleosomes covering these sequences in vivo undergo conformational transitions that play crucial roles in the gene activation process (*45*, *46*, *66*). Sea urchin 5S rDNA (*47*) is a widely used template for in vitro nucleosome studies (*48*), which we used as a standard of comparison.

All three sequences form nucleosomes with similar gel mobilities and salt stabilities at moderate NaCl concentrations. However, some consistent variations in properties among the three types of nucleosomes are detected. The 5S nucleosome has a 40% higher diffusion coefficient (Figure 7 and Table 1) and a 15−30% higher energy transfer efficiency, in gels or in solution (Figures 2 and 3 and Table 1), than MMTV-B or *GAL10* nucleosomes. The FRET signal from 5S nucleosomes is undiminished by dilution to 100 pM or heating to 42 °C, whereas those treatments reduce the magnitude of the FRET signal from MMTV-B and *GAL10* nucleosomes by 10−35% (Figures 5 and 6). 5S nucleosomes maintain a higher level of energy transfer than *GAL10* and MMTV-B nucleosomes at elevated concentrations of NaCl (≥600 mM), and the three also behave differently at low NaCl concentrations (Figure 4). The dilution, heating, and high-salt results indicate that 5S nucleosomes are less affected and are therefore more stable than MMTV or *GAL10* nucleosomes to those treatments. These variations are detected in nucleosomes containing DNA that was fluorescently labeled with the same dyes in the same way and

reconstituted with the same histones; only the sequence of the DNA varies (lengths are similar). Therefore, these results indicate that there are clear and readily detectable DNA sequence-associated structure and stability differences among these three types of nucleosomes, the hypothesis we wished to test in these experiments. Such differences should be independent of the histones used to make the nucleosomes, and this is the case (cf. Figure 4b, inset).

The nucleosome samples were used directly as reconstituted due to sample limitations. However, their slight heterogeneity [minor amounts of free DNA and higher-molecular weight material (Figure 2)] cannot undermine the conclusion that the intrinsic properties of these mononucleosomes vary. First, FRET efficiency determinations performed directly on nucleosome bands in gels show the same types of differences detected in the whole sample (in solution). Second, mononucleosomes eluted from gels show the same types of single-molecule FRET efficiency and FCS variations (data not shown) as seen for the unfractionated samples (Figures 3 and 7 and Table 1). Thus, the FRET efficiency and FCS differences are clearly intrinsic properties of the three mononucleosomes. Moreover, free DNA gives no FRET signal (*30*) and thus cannot contribute to the normalized FRET changes shown in Figures 4−7, and the similar (and minor) amounts of higher-molecular weight material seen in all the samples are unlikely to account for the substantial stability variations (Figures 4−7).

All three sequences are known to position nucleosomes (*12*, *20*, *45*, *49*−*52*), and we find one major occupied position for each, based on gel analyses (Figure 2). Also, gel profiles and nucleosome features are unchanged (data not shown) when samples are heated to maximize positioning equilibria (*67*). The primers used to synthesize the DNA fragments used in the reconstitution were chosen so that the fluorophores would lie in similar positions, ∼30 bp from each terminus in the various nucleosomes, based on the prior nucleosome positioning studies [5S (*51*, *52*), MMTV-B (*12*, *58*), and *GAL10* (reviewed in ref *45*)]. A slightly different MMTV-B position has been suggested (cf. ref *20*). That position would place the probes 10 and ∼50 bp from the MMTV-B nucleosome termini. Since DNA lability decreases with distance from the nucleosome terminus (cf. ref *27*), such a probe location could itself produce differences in the FRET responses of MMTV-B versus 5S nucleosomes and thus contribute to the observed variations. However, the observation of only partial FRET changes in MMTV-B nucleosomes at 42 °C (20%, Figure 5) argues against the 10/50 position; the release of 20−25 bp of DNA from each terminus at 42 °C (*64*) should drastically increase the average fluorophore separation and cause a major or even complete FRET loss at those temperatures if one fluorophore was located 10 bp from the terminus. The observed FRET loss (20%) would correspond to only a modest increase in average probe separation [a couple of nanometers at most, assuming the probes are ∼1.5 nm apart in the nucleosome at 25 °C (*1*) and assuming static changes]. Also, the dynamic nature of DNA−histone associations in terminal nucleosome regions, even at room temperature (*27*, *68*, *69*), would be expected to produce more significant conformational (and therefore FRET) changes at lower salt concentrations and temperatures, if one dye was located 10 bp from a terminus. Instead, the changes occur under conditions that were shown previously (*7*, *70*) to cause significant nucleosome changes (see also below). Future experiments will involve moving the fluorophores around on the DNA, to see how the fluorescence behavior varies with nucleosome location, which will address this possibility (10/50 probe locations in MMTV) and other (see below) issues.

Physical interpretations of the types of FRET variations detected in these studies can be complicated and somewhat uncertain, but several possibilities are suggested by the nature of the changes. The diffusion coefficient (FCS) differences indicate that 5S nucleosomes have a more compact conformation than MMTV or *GAL10* nucleosomes under ambient conditions, perhaps reflecting the strong histone binding properties of the 5S sequence. FRET efficiency differences indicate variations in the average distance between the two fluorophores in the nucleosome structure. These could arise from static differences, such as in the precise path of nucleosomal DNA around the octamer, or conformational dynamics differences or other causes (see also below).

The observed variations (FRET, FCS, or stability) could also be caused, at least in part, by differences in intrinsic DNA features in these three sequences. For example, recent work has demonstrated the importance of DNA twist defects in nucleosomes (*71*). This could be a source of variation in structure or stability features. Also, *GAL10* and MMTV-B sequences both have intrinsic bends near the centers of the DNA fragments (*45*, *50*); these may also contribute to the MMTV-B and *GAL10* versus 5S differences. For example, bending and bendability are known to affect the DNA−histone interaction (*72*).

It is also noteworthy that the salt-, concentration-, and temperature-dependent stability differences noted between 5S and MMTV-B or *GAL10* nucleosomes are observed under conditions that cause dissociation of the H2A−H2B dimer or release of terminal DNA from the nucleosome. For example, at NaCl concentrations above 500 mM (*7*) and as nucleosomes are diluted to nanomolar nucleosome concentrations (*70*), there is major dissociation of H2A−H2B dimers from the nucleosome. At temperatures around 40 °C, terminal DNA is known to be released (*64*). The major stability variations we observe occur at NaCl concentrations of ≥600 mM, at subnanomolar nucleosome concentrations, and as temperatures approach 40 °C, all conditions similar to those shown to cause H2A−H2B and terminal DNA release. This raises the possibility (but of course does not prove) that the stability variations among these nucleosomes may be associated with these two processes, which themselves may be related since H2A−H2B dimers interact significantly with the terminal regions of nucleosomal DNA (*1*). The partial nature of the temperature- and concentration-dependent changes we observe (at most 35%) is consistent with such partial changes in nucleosome structure. It is clear that nucleosomal DNA can affect the H2A−H2B dimer−H3−H4 tetramer interaction and thus the ease with which H2A−H2B dimers are lost because in the absence of DNA under these conditions, the octamer dissociates into H2A−H2B dimers and an H3−H4 tetramer (*73*). Thus, it is possible that sequence features of DNA could affect that interaction.

Differences in the extents of H2A−H2B dissociation and DNA release could be responsible for the stability variations. However, 5S nucleosomes show no FRET loss with dilution (Figure 6) even though they were reported to release H2A−

H2B dimers under these conditions (*70*). Therefore, these variations could (also) involve differences in how well effects are propagated within the nucleosome, from the terminal regions where the changes might be occurring to the more internal regions where our fluorophores are most likely to be located. Ease of propagation ought to depend on the strength of the DNA−histone interaction, and 5S DNA−histone binding is stronger than MMTV-B−DNA binding (F. J. Solis et al., manuscript submitted for publication). Such effects could also be involved in the observed salt- and temperature-dependent stability variations. Moving the probes around in the nucleosome should help answer this question.

Dissociation of the H2A−H2B dimer from the nucleosome is emerging as a functionally important process. H2A−H2B dimers are rapidly exchanged in vivo (*74*), and H2A−H2B dimers have been shown to be released during the interactions of nucleosomes with RNA polymerase (*75*), the transcription elongation factor FACT (*76*), and ATP-dependent nucleosome remodeling complexes (*25*, *77*, *78*). The possible association of sequence-dependent nucleosome variations with the release of H2A−H2B dimers is thus intriguing.

REFERENCES

1. Luger, K., Mader, A. W., Richmond, R. K., Sargent, D. F., and Richmond, T. J. (1997) Crystal structure of the nucleosome core particle at 2.8 Å resolution, *Nature 18*, 251−260.
2. Van Holde, K., Zlatanova, J., Arents, G., and Moudrianakis, E. (1995) in *Chromatin Structure and Gene Expression* (Elgin, S. C., Ed.) 1st ed., pp 1−21, Oxford University Press, Oxford, U.K.
3. Khorasanizadeh, S. (2004) The nucleosome: From genomic organization to genomic regulation, *Cell 116*, 259−272.
4. Peterson, C., and Laniel, M. A. (2004) Histones and histone modifications, *Curr. Biol. 14*, R546−R551.
5. De la Cruz, X., Lois, S., Sánchez-Molina, S., and Martínez-Balbás, M. (2005) Do protein motifs read the histone code? *BioEssays 27*, 164−175.
6. Kamakaka, R. T., and Biggins, S. (2005) Histone variants: Deviants? *Genes Dev. 19*, 295−310.
7. Park, Y. J., Dyer, P. N., Tremethick, D. J., and Luger, K. (2004) A new fluorescence resonance energy transfer approach demonstrates that the histone variant H2AZ stabilizes the histone octamer within the nucleosome, *J. Biol. Chem. 279*, 24274−24282.
8. Bao, Y., Konesky, K., Park, Y. J., Rosu, S., Dyer, P. N., Rangasamy, D., Tremethick, D. J., Laybourn, P. J., and Luger, K. (2004) Nucleosomes containing the histone variant H2A.Bbd organize only 118 base pairs of DNA, *EMBO J. 23*, 3314−3324.
9. Lohr, D., Kovacic, R. T., and Van Holde, K. E. (1977) Quantitative analysis of the digestion of yeast chromatin by staphylococcal nuclease, *Biochemistry 16*, 463−471.
10. Wallrath, L. L., Lu, Q., Granok, H., and Elgin, S. C. (1994) Architectural variations of inducible eukaryotic promoters: Preset and remodeling chromatin structures, *BioEssays 16*, 165−170.
11. Lu, Q., Wallrath, L. L., and Elgin, S. C. (1994) Nucleosome positioning and gene regulation, *J. Cell. Biochem. 55*, 83−92.
12. Fragoso, G., John, S., Roberts, M. S., and Hager, G. L. (1995) Nucleosome positioning on the MMTV LTR results from the frequency-biased occupancy of multiple frames, *Genes Dev. 9*, 1933−1947.
13. Lohr, D. (1997) Nucleosome transactions on the promoters of the yeast GAL and PHO genes, *J. Biol. Chem. 272*, 26795−26798.
14. Bernstein, B. E., Liu, C. L., Humphrey, E. L., Perlstein, E. O., and Schreiber, S. L. (2004) Global nucleosome occupancy in yeast, *Genome Biol. 5*, R62.
15. Sogo, J. M., Stahl, H., Koller, T., and Knippers, R. (1986) Structure of replicating simian virus 40 minichromosomes. The replication fork, core histone segregation and terminal structures, *J. Mol. Biol. 189*, 189−204.
16. Lohr, D., and Torchia, T. (1988) Structure of the chromosomal copy of yeast ARS1, *Biochemistry 27*, 3961−3965.
17. Thoma, F. (1992) Nucleosome positioning, *Biochim. Biophys. Acta 1130*, 1−19.
18. Narlikar, G. J., Fan, H. Y., and Kingston, R. E. (2002) Cooperation between complexes that regulate chromatin structure and transcription, *Cell 108*, 475−487.
19. Shrader, T. E., and Crothers, D. M. (1990) Effects of DNA sequence and histone-histone interactions on nucleosome placement, *J. Mol. Biol. 216*, 69−84.
20. Flaus, A., and Richmond, T. J. (1998) Positioning and stability of nucleosomes on MMTV 3′LTR sequences, *J. Mol. Biol. 275*, 427−441.
21. Thastrom, A., Lowary, P. T., Widlund, H. R., Cao, H., Kubista, M., and Widom, J. (1999) Sequence motifs and free energies of selected natural and non-natural nucleosome positioning DNA sequences, *J. Mol. Biol. 288*, 213−229.
22. Wu, C., and Travers, A. (2005) Relative affinities of DNA sequences for the histone octamer depend strongly upon both the temperature and octamer concentration, *Biochemistry 44*, 14329−14334.
23. Giresi, P. G., Gupta, M., and Lieb, J. D. (2006) Regulation of nucleosome stability as a mediator of chromatin function, *Curr. Opin. Genet. Dev. 16*, 171.
24. Krajewski, W. A. (2002) Histone acetylation status and DNA sequence modulate ATP-dependent nucleosome repositioning, *J. Biol. Chem. 277*, 14509−14513.
25. Vicent, G. P., Nacht, A. S., Smith, C. L., Peterson, C. L., Dimitrov, S., and Beato, M. (2004) DNA instructed displacement of histones H2A and H2B at an inducible promoter, *Mol. Cell 16*, 439−452.
26. Widlund, H. R., Vitolo, J. M., Thiriet, C., and Hayes, J. J. (2000) DNA sequence-dependent contributions of core histone tails to nucleosome stability: Differential effects of acetylation and proteolytic tail removal, *Biochemistry 39*, 3835−3841.
27. Anderson, J. D., and Widom, J. (2000) Sequence and position-dependence of the equilibrium accessibility of nucleosomal DNA target sites, *J. Mol. Biol. 296*, 979−987.
28. Sivolob, A., Lavelle, C., and Prunell, A. (2003) Sequence-dependent nucleosome structural and dynamic polymorphism. Potential involvement of histone H2B N-terminal tail proximal domain, *J. Mol. Biol. 326*, 49−63.
29. Gemmen, G. J., Sim, R., Haushalter, K. A., Ke, P. C., Kadonaga, J. T., and Smith, D. E. (2005) Forced unraveling of nucleosomes assembled on heterogeneous DNA using core histones, NAP-1, and ACF, *J. Mol. Biol. 351*, 89−99.
30. Lovullo, D., Daniel, D., Yodh, J., Lohr, D., and Woodbury, N. W. (2005) A fluorescence resonance energy transfer-based probe to monitor nucleosome structure, *Anal. Biochem. 341*, 165−172.
31. Antikainen, N. M., Smiley, R. D., Benkovic, S. J., and Hammes, G. G. (2005) Conformation coupled enzyme catalysis: Single-molecule and transient kinetics investigation of dihydrofolate reductase, *Biochemistry 44*, 16835−16843.
32. Eggeling, C., Widengren, J., Brand, L., Schaffer, J., Felekyan, S., and Seidel, C. A. (2006) Analysis of photobleaching in single-molecule multicolor excitation and Forster resonance energy transfer measurements, *J. Phys. Chem. A 110*, 2979−2995.
33. Ha, T., Ting, A. Y., Liang, J., Caldwell, W. B., Deniz, A. A., Chemla, D. S., Schultz, P. G., and Weiss, S. (1999) Single-molecule fluorescence spectroscopy of enzyme conformational dynamics and cleavage mechanism, *Proc. Natl. Acad. Sci. U.S.A. 96*, 893−898.
34. Kuzmenkina, E. V., Heyes, C. D., and Nienhaus, G. U. (2006) Single-molecule FRET study of denaturant induced unfolding of RNase H, *J. Mol. Biol. 357*, 313−324.
35. Laurence, T. A., Kong, X., Jager, M., and Weiss, S. (2005) Probing structural heterogeneities and fluctuations of nucleic acids and denatured proteins, *Proc. Natl. Acad. Sci. U.S.A. 102*, 17348−17353.
36. Laurence, T. A., and Weiss, S. (2003) Analytical chemistry. How to detect weak pairs, *Science 299*, 667−668.
37. Moerner, W. E. (2002) A dozen years of single-molecule spectroscopy in physics, chemistry, and biophysics, *J. Phys. Chem. B 106*, 910−927.
38. Rasnik, I., McKinney, S. A., and Ha, T. (2005) Surfaces and orientations: Much to FRET about? *Acc. Chem. Res. 38*, 542−548.
39. Sabanayagam, C. R., Eid, J. S., and Meller, A. (2005) Long time scale blinking kinetics of cyanine fluorophores conjugated to DNA and its effect on Forster resonance energy transfer, *J. Chem. Phys. 123*, 224708.
40. Schuler, B., Lipman, E. A., and Eaton, W. A. (2002) Probing the free-energy surface for protein folding with single-molecule fluorescence spectroscopy, *Nature 419*, 743−747.

41. Sosa, H., Peterman, E. J., Moerner, W. E., and Goldstein, L. S. (2001) ADP-induced rocking of the kinesin motor domain revealed by single-molecule fluorescence polarization microscopy, *Nat. Struct. Biol. 8*, 540−544.
42. Weiss, S. (2000) Measuring conformational dynamics of biomolecules by single molecule fluorescence spectroscopy, *Nat. Struct. Biol. 7*, 724−729.
43. Zhuang, X., Kim, H., Pereira, M. J., Babcock, H. P., Walter, N. G., and Chu, S. (2002) Correlating structural dynamics and function in single ribozyme molecules, *Science 296*, 1473−1476.
44. Tomschik, M., Zheng, H., van Holde, K., Zlatanova, J., and Leuba, S. H. (2005) Fast, long-range, reversible conformational fluctuations in nucleosomes revealed by single-pair fluorescence resonance energy transfer, *Proc. Natl. Acad. Sci. U.S.A. 102*, 3278−3283.
45. Bash, R., and Lohr, D. (2001) Yeast chromatin structure and regulation of GAL gene expression, *Prog. Nucleic Acid Res. Mol. Biol. 65*, 197−259.
46. Hager, G. L. (2001) Understanding nuclear receptor function: From DNA to chromatin to the interphase nucleus, *Prog. Nucleic Acid Res. Mol. Biol. 66*, 279−305.
47. Simpson, R. T., and Stafford, D. W. (1983) Structural features of a phased nucleosome core particle, *Proc. Natl. Acad. Sci. U.S.A. 80*, 51−55.
48. Hansen, J. C. (2002) Conformational dynamics of the chromatin fiber in solution: Determinants, mechanisms, and functions, *Annu. Rev. Biophys. Biomol. Struct. 31*, 361−392.
49. Perlmann, T., and Wrange, O. (1988) Specific glucocorticoid receptor binding to DNA reconstituted in a nucleosome, *EMBO J. 7*, 3073−3079.
50. Pina, B., Bruggemeier, U., and Beato, M. (1990) Nucleosome positioning modulates accessibility of regulatory proteins to the mouse mammary tumor virus promoter, *Cell 60*, 719−731.
51. Dong, F., Hansen, J. C., and van Holde, K. E. (1990) DNA and protein determinants of nucleosome positioning on sea urchin 5S rRNA gene sequences in vitro, *Proc. Natl. Acad. Sci. U.S.A. 87*, 5724−5728.
52. Meersseman, G., Pennings, S., and Bradbury, E. M. (1991) Chromatosome positioning on assembled long chromatin. Linker histones affect nucleosome placement on 5 S rDNA, *J. Mol. Biol. 220*, 89−100.
53. Bash, R. C., Vargason, J. M., Cornejo, S., Ho, P. S., and Lohr, D. (2001) Intrinsically bent DNA in the promoter regions of the yeast GAAL1−10. and GAL80 genes, *J. Biol. Chem. 276*, 861−866.
54. Fletcher, T. M., Ryu, B. W., Baumann, C. T., Warren, B. S., Fragoso, G., John, S., and Hager, G. L. (2000) Structure and dynamic properties of a glucocorticoid receptor-induced chromatin transition, *Mol. Cell. Biol. 20*, 6466−6475.
55. Bash, R. C., Yodh, J., Lyubchenko, Y., Woodbury, N., and Lohr, D. (2001) Population analysis of subsaturated 172-12 nucleosomal arrays by atomic force microscopy detects nonrandom behavior that is favored by histone acetylation and short repeat length, *J. Biol. Chem. 276*, 48362−48370.
56. Yodh, J. G., Lyubchenko, Y. L., Shlyakhtenko, L. S., Woodbury, N., and Lohr, D. (1999) Evidence for nonrandom behavior in 208-12 subsaturated nucleosomal array populations analyzed by AFM, *Biochemistry 38*, 15756−15763.
57. Luger, K., Rechsteiner, T. J., and Richmond, T. J. (1999) Expression and purification of recombinant histones and nucleosome reconstitution, *Methods Mol. Biol. 119*, 1−16.
58. Fragoso, G., Pennie, W. D., John, S., and Hager, G. L. (1998) The position and length of the steroid-dependent hypersensitive region in the mouse mammary tumor virus long terminal repeat are invariant despite multiple nucleosome B frames, *Mol. Cell. Biol. 18*, 3633−3644.
59. Krichevsky, O., and Bonnet, G. (2002) Fluorescence correlation spectroscopy: The technique and its applications, *Rep. Prog. Phys. 65*, 251−297.
60. Neubauer, B., and Horz, W. (1989) Analysis of nucleosome positioning by in vitro reconstitution, *Methods Enzymol. 170*, 630−644.
61. Pennings, S. (1999) Nucleoprotein gel assays for nucleosome positioning and mobility, *Methods Enzymol. 304*, 298−312.
62. Czarnota, G. J., and Ottensmeyer, F. P. (1996) Structural states of the nucleosome, *J. Biol. Chem. 271*, 3677−3683.
63. Mangenot, S., Leforestier, A., Vachette, P., Durand, D., and Livolant, F. (2002) Salt-induced conformation and interaction changes of nucleosome core particles, *Biophys. J. 82*, 345−356.
64. Van Holde, K. (1989) *Chromatin*, Springer-Verlag, Berlin.
65. Davey, C. A., Sargent, D. F., Luger, K., Maeder, A. W., and Richmond, T. J. (2002) Solvent mediated interactions in the structure of the nucleosome core particle at 1.9 angstrom resolution, *J. Mol. Biol. 319*, 1097−1113.
66. Lohr, D. (1984) Organization of the GAL1-GAL10 intergenic control region chromatin, *Nucleic Acids Res. 12*, 8457−8474.
67. Flaus, A., Luger, K., Tan, S., and Richmond, T. J. (1996) Mapping nucleosome position at single base-pair resolution by using site-directed hydroxyl radicals, *Proc. Natl. Acad. Sci. U.S.A. 93*, 1370−1375.
68. Li, G., and Widom, J. (2004) Nucleosomes facilitate their own invasion, *Nat. Struct. Mol. Biol. 11*, 763−769.
69. Li, G., Levitus, M., Bustamante, C., and Widom, J. (2005) Rapid spontaneous accessibility of nucleosomal DNA, *Nat. Struct. Mol. Biol. 12*, 46−53.
70. Claudet, C., Angelov, D., Bouvet, P., Dimitrov, S., and Bednar, J. (2005) Histone octamer instability under single molecule experiment conditions, *J. Biol. Chem. 280*, 19958−19965.
71. Edayathumangalam, R. S., Weyermann, P., Dervan, P. B., Gottesfeld, J. M., and Luger, K. (2005) Nucleosomes in solution exist as a mixture of twist-defect states, *J. Mol. Biol. 345*, 103−114.
72. Widom, J. (2001) Role of DNA sequence in nucleosome stability and dynamics, *Q. Rev. Biophys. 34*, 269−324.
73. Luger, K. (2003) Structure and dynamic behavior of nucleosomes, *Curr. Opin. Genet. Dev. 13*, 127−135.
74. Kimura, H., and Cook, P. R. (2001) Kinetics of core histones in living human cells: Little exchange of H3 and H4 and some rapid exchange of H2B, *J. Cell Biol. 153*, 1341−1353.
75. Studitsky, V. M., Walter, W., Kireeva, M., Kashlev, M., and Felsenfeld, G. (2004) Chromatin remodeling by RNA polymerases, *Trends Biochem. Sci. 29*, 127−135.
76. Belotserkovskaya, R., and Reinberg, D. (2004) Facts about FACT and transcript elongation through chromatin, *Curr. Opin. Genet. Dev. 14*, 139−146.
77. Bruno, M., Flaus, A., Stockdale, C., Rencurel, C., Ferreira, H., and Owen-Hughes, T. (2003) Histone H2A/H2B dimer exchange by ATP-dependent chromatin remodeling activities, *Mol. Cell 12*, 1599−1606.
78. Bash, R., Wang, H., Anderson, C., Yodh, J., Hager, G., Lindsay, S. M., and Lohr, D. (2006) AFM imaging of protein movements: Histone H2A-H2B release during nucleosome remodeling, *FEBS Lett. 580*, 4757−4761.

BI061289L